CHEMMEDCHEM

CHEMISTRY ENABLING DRUG DISCOVERY

Accepted Article

Title: Optimization of LpxC Inhibitors for Antibacterial Activity and Cardiovascular Safety

Authors: Frederick Cohen, James B. Aggen, Logan D. Andrews, Zahra Assar, Jen Boggs, Taylor Choi, Paola Dozzo, Ashton N. Easterday, Cat M. Haglund, Darin J. Hildebrandt, Melissa C. Holt, Kristin Joly, Adrian Jubb, Zeeshan Kamal, Timothy R. Kane, Andrei W. Konradi, Kevin M. Krause, Martin S. Linsell, Timothy D. Machajewski, Olga Miroshnikova, Heinz E. Moser, Vincent Nieto, Thu Phan, Craig Plato, Alisa W. Serio, Julie Seroogy, Anton Shakhmin, Adam J. Stein, Alex D. Sun, Serguei Sviridov, Zhan Wang, Kenneth Wlasichuk, Wen Yang, Xiaoming Zhou, Hai Zhu, and Ryan T. Cirz

To be cited as: *ChemMedChem* 10.1002/cmdc.201900287

Link to VoR: http://dx.doi.org/10.1002/cmdc.201900287

A Journal of

ChemPubSoc Europe

WILEY-VCH

www.chemmedchem.org

FULL PAPER WILEY-VCH

Optimization of LpxC Inhibitors for Antibacterial Activity and Cardiovascular Safety

Frederick Cohen*[a], James B. Aggen[a], Logan D. Andrews[a], Zahra Assar[b], Jen Boggs[a], Taylor Choi[a], Paola Dozzo[a], Ashton N. Easterday[a], Cat M. Haglund[a], Darin J. Hildebrandt[a], Melissa C. Holt[b], Kristin Joly[c], Adrian Jubb[a], Zeeshan Kamal[d], Timothy R. Kane[a], Andrei W. Konradi[e], Kevin M. Krause[a], Martin S. Linsell[a], Timothy D. Machajewski[a], Olga Miroshnikova[d], Heinz E. Moser[a], Vincent Nieto[a], Thu Phan[d], Craig Plato[c], Alisa W. Serio[a], Julie Seroogy[a], Anton Shakhmin[d], Adam J. Stein[b], Alex D. Sun[d], Serguei Sviridov[d], Zhan Wang[d], Kenneth Wlasichuk[a], Wen Yang[d], Xiaoming Zhou[f], Hai Zhu[d], Ryan T. Cirz*[a]

[a] Dr. F. Cohen 0000-0003-2229-3900, Dr. J. Aggen, Dr. L. Andrews 0000-0002-5092-4530 , J. Boggs, Dr. T. Choi, Dr. P. Dozzo, A. Easterday, Dr. C. Haglund, D. Hildebrandt, Dr. A. Jubb, T. Kane, K. Krause, M. Linsell, Dr. T. Machajewski, Dr. H. Moser, Dr. V. Nieto, Dr. A. Serio., J. Seroogy, K. Wlasichuk, Dr. R. Cirz 0000-0002-9848-7421
Achaogen Inc.
1 Tower Place, Suite 400, South San Francisco, CA 94080, United States
E-mail: frederickcohen2017@gmail.com
ryancirz@gmail.com

[b] Dr. Z. Assar 0000-0001-6008-6203, M. Holt 0000-0002-7883-924X, Dr. A. Stein 0000-0002-9948-0870
Cayman Chemical Co.
1180 E. Ellsworth, Ann Arbor, MI 48108, United States

[c] K. Joly, Dr. C. Plato
Plato BioPharma, Inc.
7581 W 103rd Ave Unit 300, Broomfield, CO 80021, United States

[d] Dr. Z. Kamal, O. Miroshnikova, T. Phan, Dr. A. Shakhmin, Dr. A. Sun, Dr. S. Sviridov, Z. Wang, Dr. W. Yang, Dr. H. Zhu
Nanosyn, Inc.
3100 Central Expressway, Santa Clara, California, 95051, United States

[e] Dr. A. Konradi
Konradi Molecular
30 Victoria Rd, Burlingame, CA 94010, United States

[f] Dr. X. Zhou
Pharmaron, Inc.
6 Tai-He Road, BDA, Beijing, 100176, China

Supporting information for this article is given via a link at the end of the document.((Please delete this text if not appropriate))

Abstract: LpxC is a Zn^{2+} deacetylase that is essential for the survival of most pathogenic Gram(–) bacteria. **ACHN-975** (N-((S)-3-amino-1-(hydroxyamino)-3-methyl-1-oxobutan-2-yl)-4-(((1R,2R)-2-(hydroxymethyl)cyclopropyl)buta-1,3-diyn-1-yl)benzamide) was the first LpxC inhibitor to reach human clinical testing and was discovered to have a dose-limiting cardiovascular toxicity of transient hypotension without compensatory tachycardia. We report here the effort beyond **ACHN-975** to discover LpxC inhibitors optimized for enzyme potency, antibacterial activity, pharmacokinetics, and cardiovascular safety. Based on overall profile, **26** (**LPXC-516**, (S)-N-(2-(hydroxyamino)-1-(3-methoxy-1,1-dioxidothietan-3-yl)-2-oxoethyl)-4-(6-hydroxyhexa-1,3-diyn-1-yl)benzamide) was chosen for further development. A phosphate prodrug of **26** was developed that provided solubility of >30 mg/mL for parenteral administration and conversion to the active drug with a $T_{1/2}$ of approximately 2 minutes. Unexpectedly, and despite our optimization efforts, the prodrug of **26** still possesses a therapeutic window insufficient to support further clinical development.

Introduction

Effective antibiotic therapy is a foundation of modern medicine. Procedures that are routine and life-saving such as coronary stents, joint and organ transplants, and cancer chemotherapy rely on effective antibiotic therapy. Due to bacterial evolution and misuse of antibiotics, we are in danger of losing this foundation.[1,2] In addition, the pipeline of new antibiotic therapies has not kept pace with the growing threat. Patients have succumbed to infections that are resistant to every approved antibiotic.[3] The combination of scientific and economic challenges behind this divergence has been reviewed.[4,5] Current estimates place the mortality due to multidrug-resistant (MDR) bacteria between 23,000 and 160,000 annually in the US alone.[1,2]

As part of an on-going effort to introduce antibiotic therapies with completely novel mechanisms of action, we pursued a research and development program aimed at bringing a novel inhibitor of the bacterial enzyme UDP-3-O-(R-3-hydroxymyristoyl)-N-acetylglucosamine deacetylase (LpxC) to patients. This enzyme catalyzes the first committed step in the synthesis of lipopolysaccharide (LPS), removal of an N-Acetyl group from the growing LPS core and is essential to most Gram-negative pathogens (Figure 1).[6] Additionally, there are no mammalian homologs of LpxC, eliminating the possibility of on-target toxicity, and increasing interest in the target.

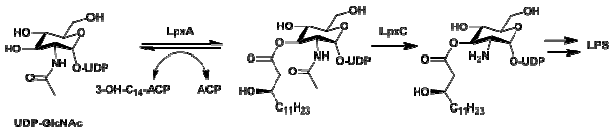

Figure 1. LpxC catalyzes the first committed step of LPS biosynthesis.

The first LpxC inhibitor to reach clinical trials from this program was **ACHN-975**. In a single-ascending dose study, we discovered a C_{max}-driven dose-limiting toxicity (DLT) of transient hypotension without tachycardia. Herein we describe our work to identify a second

clinical candidate with a wider therapeutic window for cardiovascular (CV) safety.

During the development of **ACHN-975** we discovered that the respiratory pathogen *Pseudomonas aeruginosa* was more sensitive to LpxC inhibition in *in vivo* models than Enterobacteriaceae species such as *Escherichia coli* and *Klebsiella pneumoniae*. Furthermore, the LpxC substrate binding pocket in Enterobacteriaceae species has a longer hydrophobic tunnel than *P. aeruginosa*. This structural difference results in a requirement for longer, more amphiphilic inhibitors, which we thought would make solving the toxicity problems more challenging. Finally, the pipeline of novel anti-pseudomonal agents is even sparser than for the Enterobacteriaceae. For these reasons, we focused our second optimization program exclusively on *P. aeruginosa*.

Results and Discussion

SAR of Bis Alkyne Scaffold. LpxC inhibitors are generally composed of three segments, a hydroxamic acid, or other bidentate metal ligand to chelate the catalytic Zn^{2+} atom, a polar moiety that occupies the sugar-binding pocket (the 'head group'), and a hydrophobic tail to fill the hydrophobic tunnel that is usually occupied by the C_{10}-C_{16} aliphatic chain in the natural substrate.[7,8] In this work, we focused on a benzamide bis-acetylene linker to span the hydrophobic tunnel and explored the effect of structural modification of the head group and of the portion of the tail that extended out of the hydrophobic tunnel. Compounds were initially evaluated for their ability to inhibit purified LpxC and anti-bacterial potency and the data are summarized in Table 1. The screening panel contained wild-type strains of *P. aeruginosa* (PAO1). To measure the ability of compounds to cross the outer membrane in *P. aeruginosa*, we added polymyxin B nonapeptide (PMBN) to permeabilize the outer membrane.[9] We used a strain of *P. aeruginosa* with its major efflux systems (MexAB-oprM, MexCD-oprJ, MexEF-oprN, and MexXY) deleted or rendered inactive to measure each compound's efflux liability.[10] We also evaluated the activity of compounds against five recent clinical isolates of *P. aeruginosa*. The geometric mean of the minimum inhibitory concentrations (MICs) of these five strains (listed as "MIC5" in Table 1) was an accurate predictor of the MIC_{90} against a larger panel of 40 clinical isolates.[11] To get an accurate estimate of the total drug levels that would be required for efficacy, we also measured plasma protein binding (PPB) as a primary assay in our testing funnel.[12] We then looked to the PPB adjusted MIC as our primary measure of activity.

We further evaluated these compounds for on-target antibacterial activity by assaying them against a strain of *P. aeruginosa* that overexpresses LpxC. All compounds in Table 1 show ≥ 8-fold increase in MIC against this strain (data not shown), indicating that they remain on-target.

SAR for LpxC Inhibition. Compounds that lack polarity at the solvent-exposed end of the tail, such as **1**, are generally potent enzyme inhibitors (IC_{50} < 1 nM) with potent antibacterial activity across species and low (≤ 4-fold) shift in MIC upon addition of PMBN, indicating high permeability across the outer membrane. Larger shifts were seen in the efflux-deficient strain (≥ 10-fold), indicating that these compounds are relatively good substrates for efflux pumps. As a group, these compounds also demonstrated a number of toxicities including cytotoxicity to endothelial cells and hemolysis of red blood cells (data not shown).

These observations led us to reduce the amphiphilic nature of the compounds by adding polar moieties on the solvent-exposed end of the hydrophobic tail. Proper placement of these groups is key to maintaining potent enzyme inhibition. For instance, **ACHN-975** containing a hydroxymethyl substituted cyclopropane is equipotent to **1**. Placing a hydroxy group close the hydrophobic tunnel as in compounds **2** and **3** results in a 10-fold increase in IC_{50}, and a concomitant loss in antibacterial activity. Analysis of the X-ray co-structure of **ACHN-975** bound to LpxC (**Figure 2**) suggested that the carbon atom attached to the second acetylene lies at the exit point of the hydrophobic tunnel. Therefore, the introduction of the polar hydroxyl group makes an unfavorable interaction with the protein. A minimum of two carbons between the acetylene and polar functionality is required to fully escape the hydrophobic tunnel and restore potent (<5 nM) enzyme inhibition (**5**). Small, hydrophobic branching at the exit of the tunnel is generally tolerated. For example, the cyclopropyl found in **ACHN-975** and the substituted azetidines found in **4** and **10** both result in potent inhibitors of the enzyme (<5 nM).

Turning our attention to the head group, we found a number of polar substituents to occupy the sugar pocket and make key interactions with the protein. For instance, **ACHN-975** makes a number of water-mediated hydrogen bonds to protein, while one of the methyl groups packs against Phe191. Inhibitors with non-basic substituents are generally less potent enzyme inhibitors (cf **5** vs **9**) unless they make additional specific interactions. The methyl sulfone replacement **15** – **17** can make additional interactions with the protein and has a similar IC_{50}. Further substitution of the sulfone afforded a vector to reach additional protein contacts. Replacing the methylsulfone of **17** (IC_{50} = 4.6 nM) with amine containing groups (**20**, IC_{50} = 4 nM and **21**, IC_{50} = 4 nM) were unable to make additional productive protein contacts. The oxetane containing substitution found in **19** makes additional hydrophobic contacts, as well as an additional hydrogen bond with the backbone amide of Phe193 Figure 3 B), and results in more than a 10-fold improvement in binding affinity (IC_{50} = 0.3 nM).

Oxetane **13** and thietanedioxides **23** – **26** were designed to interact with Lys238. As such, modification of the dimethyl of **4** (IC_{50} = 2 nM) to the oxetane, **13** (IC_{50} = 0.76 nM) resulted in a 2–3-fold increase in LpxC inhibition. Furthermore, introduction of the thiethanedioxide resulted in more than a 10-fold increase in LpxC inhibition (**22**, IC_{50} = 10 nM; **26**, IC_{50} 0.71 nM). In this case, the quaternary methoxy substitution was optimal. The single atom change of carbon for oxygen (**24**, IC_{50} = 4.3 nM) resulted in a 5-fold loss of binding affinity. Modeling studies suggested this was the result of a conformation change effect. Decreasing the size from ethyl to a methyl group (**23**, IC_{50} = 3.5 nM) did not substantially improve inhibition and increasing the size to a cyclopropyl (**25**, IC_{50} = 1.6 nM), while increasing the hydrophobic interactions, was still 2-fold higher than the methoxy group.

Antibacterial Activity. Consistent and predictable structure-antibacterial activity relationships are made more difficult due to the multitude of effects that play a role in the ability of an inhibitor to get to the target location. Often, a narrow window of physicochemical parameters defines the ability of a molecule to cross the outer membrane via porin, be effluxed by efflux pumps, and cross the inner membrane to gain access to the target in the cytoplasm. Therefore, it is not always the case that a compound with a potent inhibitory activity will result in acceptable MICs. By using the engineered strains of *P. aeruginosa* described above, either with or without the addition of PMBN, we are able to glean important information about the properties of the molecule that improve the likelihood of target engagement.

Some trends emerge from this work. Firstly, compounds from this scaffold were generally highly permeable across the outer membrane, with MIC shifts of <5 upon PMBN addition. Exceptions to this trend include **8, 16** and **19**, which lack a basic amine. These observations are consistent with other work in the field, which found that compounds containing a basic amine had higher cellular accumulation than non-basic compounds.[13, 14] For example, the ratio of the parental to pump knock-out *P. aeruginosa* strain is 8.6 for amine containing head group **5**, but 20 for the hydroxyl containing head group, **9**, and 39 for the sulphone containing head group, **17**. Reinstalling a basic group on the tail of compounds with non-basic head groups removes some of the efflux liability as demonstrated by the comparison of **9** (non-basic head and tail, ratio 20) with **12** (non-basic head, basic tail, ratio 11).

Rat cardiovascular (CV) Safety. To screen compounds for hemodynamic effects, we developed a high content assay in rats. Briefly, 4 male Sprague-Dawley (SD) rats were anesthetized with isoflurane. The femoral artery was cannulated and interfaced with a pre-calibrated pressure transducer for continuous collection of heart rate and blood pressure. The right femoral vein of each rat was cannulated for infusion of test article, and the left jugular vein was cannulated for collection of toxicokinetic samples. After equilibration, all animals

Table 1. Structure, Potency, and Activity of LpxC Inhibitors.

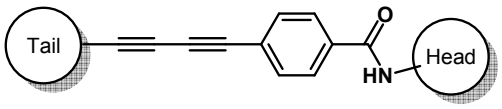

Compound	Head	Tail	LpxC IC_{50} (nM)	MIC[f] (μg/mL) PAO1	PAO1 +PMBN	PAO1 Δ efflux	PAO1 Δ efflux +PMBN	MIC5[e]	PPB h/r (% free)	MIC5/fu (h)
1			0.62	0.048	0.017	0.0041	0.0017	0.16	7/ND	2.3
ACHN-975		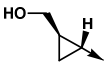	0.68	0.061	0.035	0.0055	0.0038	0.38	13/13[a]	3.0
2	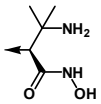		19	0.71	0.63	0.11	0.079	3.5	72/77[b,c]	4.9
3			12	1.1	1	0.22	0.16	8.8	72/77[b,c]	12
4		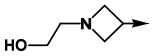	2.2	0.41	0.79	0.062	0.079	2.0	41/51[a]	4.9
5			2.2	0.12	0.12	0.014	0.013	0.81	54/49[b]	1.5
6	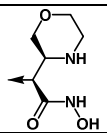	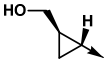	1.8	0.25	0.063	0.013	0.0039	1.1	15/14[a]	7.3
7	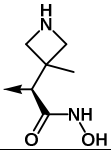		19	2	4	0.25	0.25	16	ND	–
8		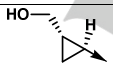	3.7	0.22	0.043	0.012	0.0032	1.1	7/9[a]	16
9 (LPXC-289)	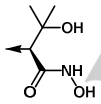		13	0.24	0.13	0.012	0.01	1.8	31/28[b]	5.8
10 (LPXC-313)		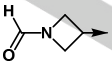	4.8	0.38	0.2	0.022	0.008	2.4	34/27[b]	7.1
11			9.1	0.66	1	0.19	0.25	4	74/59[b]	5.4
12		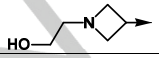	2.7	0.3	0.25	0.027	0.039	2.1	49/49[a]	4.3
13	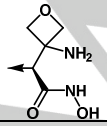	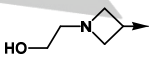	0.76	0.5	0.35	0.031	0.031	3.7	51/54[a]	7.3
14	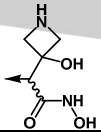		53	6	8	0.5	0.35	31	37/40[a]	84

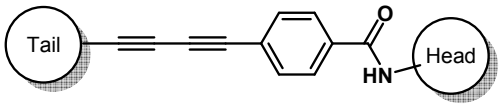

Com pound	Head	Tail	LpxC IC_{50} (nM)	MIC[f] (μg/mL) PAO1	PAO1 +PMBN	PAO1 Δ efflux	PAO1 Δ efflux +PMBN	MIC5[e]	PPB h/r (% free)	MIC5/fu (h)
15	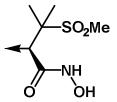	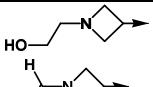	0.63	0.5	0.25	0.026	0.016	4	39/42[a]	10
16		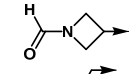	1.4	0.5	0.018	0.031	0.0039	3.4	40/26[a]	8.5
17			4.6	0.38	0.11	0.0098	0.0025	2.4	31/29	7.7
18	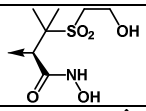	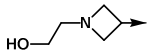	5.3	4	2	0.13	0.063	24	ND	–
19	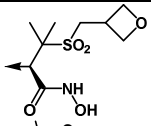		0.3	2	0.25	0.061	0.0049	9	21/23	43
20	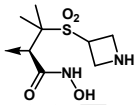		4	8	4	0.25	0.13	32	ND	–
21	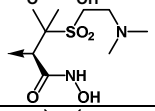		4	0.63	0.35	0.044	0.025	4.4	28/25[a]	16
22	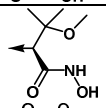		10	0.28	0.098	0.012	0.0086	1.9	34/31[a]	5.6
23	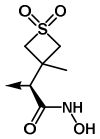		3.5	0.5	0.25	0.022	0.0078	2.8	31/23[a]	9
24	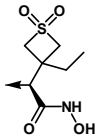		4.3	0.5	0.25	0. 022	0.011	2.5	24/20[a]	10
25	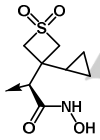		1.6	0.5	0.25	0.022	0.0078	2.6	21/14[a]	12
26 (LPXC-516)	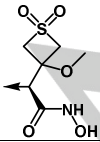		0.71	0.51	0.28	0.027	0.0081	2.3	31/25[a]	7.4
27	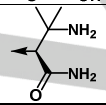	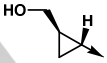	>1000			na			nd/15	

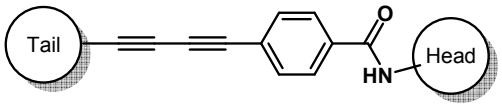

Com pound	Head	Tail	LpxC IC_{50} (nM)	MIC[f] (μg/mL) PAO1	PAO1 +PMBN	PAO1 Δ efflux	PAO1 Δ efflux +PMBN	MIC5[e]	PPB h/r (% free)	MIC5/fu (h)
28	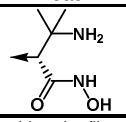	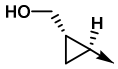	70[d]			nd			nd/14	

[a] Determined by ultrafiltration, r = rat, h = human; [b] determined by equilibrium dialysis; [c]determined for a 1:1 mixture of **2** and **3**. [d] 98% *ee*. [e] Geometric mean of five MICs, run in at least duplicate. [f] Geometric mean of MIC, run in at least duplicate.

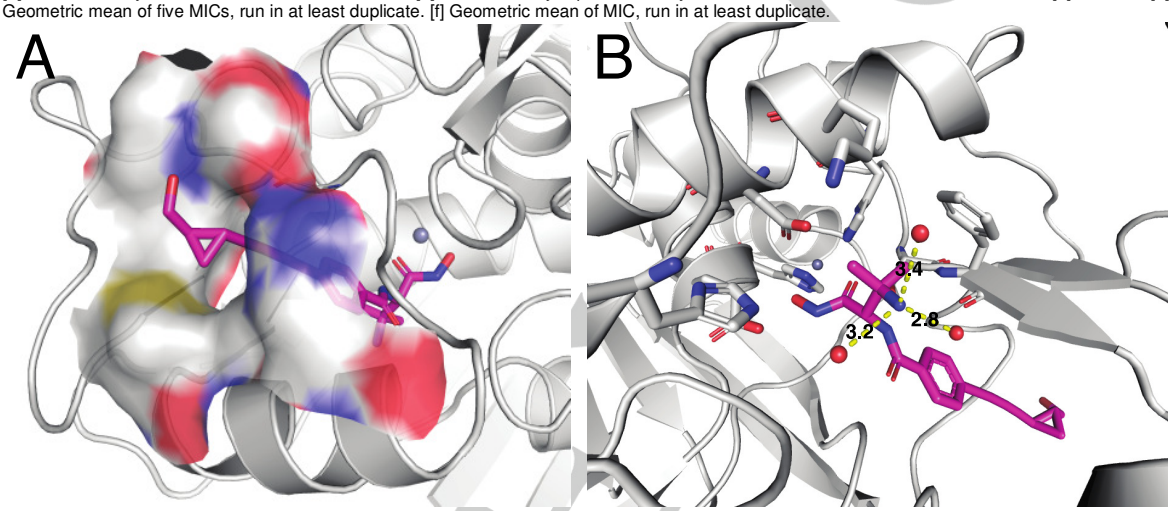

Figure 2. Structure of ACHN-975 co-crystallized with *P. aeruginosa* LpxC at a resolution of 2.2 Å (PDB 6MOO). (A) The hydroxamate moiety of **ACHN-975** (magenta) at the head group of the molecule is observed coordinating the active site Zn^{2+} ion (grey sphere) and the tail side of the molecule extends through a hydrophobic tunnel. The hydroxymethyl cyclopropyl tail group protrudes entirely out of the surface of the tunnel exit. (B) A view of **ACHN-975** within the active site. Three crystallographic water molecules shown as red spheres are in position to accept hydrogen bonds from the amine-containing head group. Distances between the oxygen atoms of the waters and the amine nitrogen atom of **ACHN-975** are labelled and highlighted by dashed yellow lines.

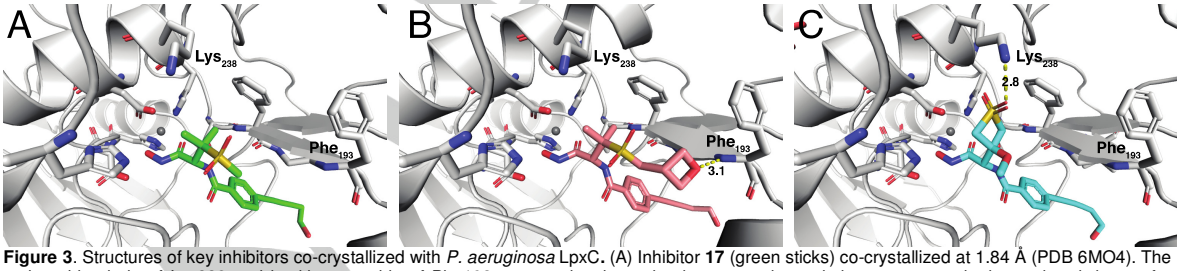

Figure 3. Structures of key inhibitors co-crystallized with *P. aeruginosa* LpxC**.** (A) Inhibitor **17** (green sticks) co-crystallized at 1.84 Å (PDB 6MO4). The amine side chain of Lys238 and backbone amide of Phe193 appeared to be to in close enough proximity to serve as hydrogen-bond donors for expanded versions of the **17** head group. (B) Inhibitor **19** (pink sticks) was co-crystallized at 1.85 Å (PDB 6MO5). The addition of the methyl oxetane moiety resulted in the oxygen atom of the oxetane positioned within hydrogen-bonding distance to the Phe193 backbone amide. (C) Inhibitor **26** (cyan sticks) was co-crystallized at 1.85 Å (PDB 6MOD). The presence of the thietane dioxide moiety results in a small conformational change of the Lys238 side chain. One of the oxygen atoms of the thietane dioxide moiety appears within hydrogen-bonding distance to the nitrogen atom of the re-positioned Lys238.

received intravenous vehicle (HPCD: 20% hydroxypropyl cyclodextrin, 250 mM Tris, in water, pH 9; or A5D: 2.5% dextrose in 20 mM acetate buffer, pH 5) for 30 minutes, followed by infusion of test article in increasing doses for 30 minutes at each dose level, or

until pre-determined stopping criteria were met (see Methods section). Toxicokinetic samples were taken at the end of the low, mid, and high doses, and at 2, 6, 10, and 30 minutes following cessation of infusion. These data were used to determine a maximum free drug concentration that resulted in < 20% change in CV parameters. This concentration was defined as the maximum tolerated concentration (MTC). Plotting these data as in Figure 4, showed that this assay reproduced the effect observed in humans in the Phase 1 trial of **ACHN-975** at the same free drug concentration (manuscript in preparation). As an estimate of the therapeutic window for CV safety, we divided the MTC by the antibacterial potency, represented by the MIC5, and these data are summarized in Table 2, along with the measured or calculated pK_a of the test compounds and the doses administered.

We systematically investigated the structure-toxicity relationships for this series of compounds using the rat CV assay. Understanding the essentiality of the hydroxamic acid to antibacterial potency and the perceived liabilities of this functionality,[15] our first modification was to remove it by reduction to the amide **27**. While this compound had no antibacterial activity, its MTC was nearly identical to **ACHN-975** (3 vs 5 μg/mL). We thus believe that it is unlikely that the hydroxamate alone is responsible for the observed toxicity. We next hypothesized that the amine functionality on the head group in proximity to the aromatic core was an ion-channel pharmacophore. This inspired us to move the amine to the distal end of the molecule in analogs **12** and **15**. These compounds had improved CV tolerability, but lost antibacterial potency, and thus still had unacceptably narrow safety windows (<30x). Neither sterically hindering the amine nor modulating the pK_a resulted in an acceptable window; any compound with a basic pK_a ≥ 6.5 demonstrated a similar effect on CV parameters. It was not until we tested compounds devoid of basic amines that we found compounds the met our criteria for CV safety (>30x). As a control for vehicle effects, **ACHN-975** was also dosed with the HPCD formulation and found to have a similar MTC.

In Vitro Pharmacology. To attempt to identify the target(s) responsible for the observed CV effects, and develop a higher-throughput assay, **ACHN-975** was profiled against a CEREP panel (Eurofins) of 123 human receptors, ion channels and enzymes at a single concentration of 10 μg/mL. Of these assays, only the site 2 sodium channel assay showed a significant signal of 50% inhibition. We followed up this result by testing a series of compounds for which we had rat *in vivo* data in the sodium channel assay at 100 μg/mL and the results are listed in Table 3. We observed no correlation between activity in this assay and the MTC or CV safety window. The caveat with this analysis is that we are comparing rat *in vivo* data to human ion channel data.

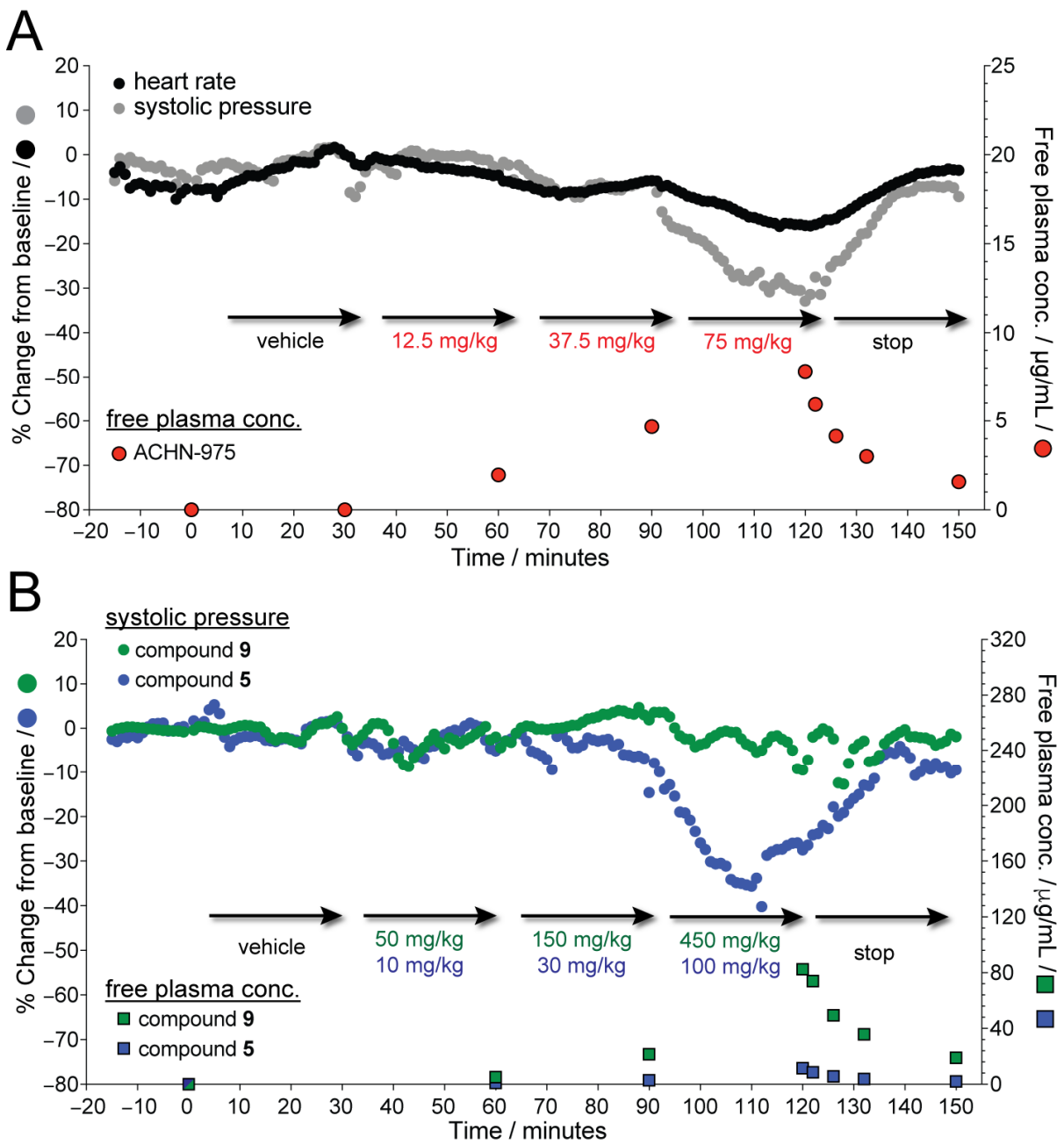

Figure 4. Rat hemodynamic assay data. (A) Effects of ACHN-975 in rats. (B) Effects of compounds **5** and **9**. Compounds **5** and **9** differ by a single heavy atom ($NH_2 \rightarrow OH$).

Table 2. Summary of Cardiovascular Safety in Rat.

Compound	pK_a	Doses (mg/kg/h)	MTC (µg/mL)[f]	MIC5 (µg/mL)	CV window
ACHN-975[a]	7.1/8.3[c]	12.5/37.5/75	5	0.38	13
27[a]	6.9[d]	50/150/450	3	NA	-
28[a]	nd	37.5/75/150	3.5	NA	-
2/3[a, e]	7.2/8.2[d]	100/200/400	26	6.2	26
4[a]	7.4/8.2[d]	75/300/450	<12	2.0	<6
5[a]	7.2/8.3[c]	50/150/450	3	0.81	4.2
6[a]	nd	50/150/450	18	1.1	16
12[a]	7.4/8.0[c]	300	12	2.1	6
15[a]	7.4/8.6	50/150/400	29	4	7
21[a]	nd	50/150/450	50	4.4	11

9[b]	9.1[c]	50/150/450	>82	1.1	>75
10[b]	7.9[c]	50/150/450	>81	2.4	>34
17[b]	7.6[c]	50/150/450	>74	2.4	>31
26[b, g]	nd	75/150/300	>73	2.3	>32

[a] Formulated in A5D (A5D: 2.5% dextrose in 20 mM acetate buffer, pH 5. [b] Formulated in HPCD: 20% hydroxypropyl cyclodextrin, 250 mM Tris, in water, pH 9. [c] Measured pKa by aqueous titration. [d] Calculated with ACD labs model with training set of measured data.1:1 [e] mixture of **2** and **3**. [f] MTC is the maximum tolerated concentration, defined as the highest measured free drug concentration that results in <20 % change in blood pressure or heart rate. [g] Tested as a racemic mixture.

We further assayed a series of compounds in a FastPatch® ion current assay in CHO cells (ChanTest). Compounds with wide or narrow CV safety windows in the rat *in vivo* assay showed no inhibition of the L-type or T-type calcium channels, Kir6.2/SURAA potassium channel, or Nav1.5 sodium channel at a concentration of 100 μg/mL (data not shown).

Table 3. Sodium Channel Binding Data

Compound	% Inhibition (100 μg/mL)	MTC[a] (μg/mL)	CV window[a]
ACHN-975	97	5	13
2/3	31	26	26
9	11	>82	>75
10	41	>81	>34
21	35	50	11

[a] from rat hemodynamic assay

Pharmacokinetics. Compounds were screened for pharmacokinetics (PK) in rats. In general, the compounds displayed moderate clearance values 20 – 40% of liver blood flow (Table 4). Two notable exceptions are **ACHN-975** and **14**. The low clearance of **14** was the inspiration for synthesis of other 4-member ring head groups that lacked basic amines, and eventually led to candidate **26**. To effect comparison between compounds of differing potency and exposure, we normalized these values by looking at the ratio of exposure (free AUC) from a constant dose to antibacterial activity as measured by the MIC5. Of the compounds that met our threshold for CV safety, **10** and **26** had the highest exposure:potency ratio. Although **9** appeared to have a wider TW, it displayed higher clearance than **10** and **26** in dog and monkey PK studies. We chose **26** for further investigation as the primary alcohol on the tail provided a more convenient handle for prodrug development relative to the tertiary alcohol on the head of **10**. Additional microbiological characterization of **ACHN-975**, **9**, **10** and **26** that also contributed to candidate selection will be described in an accompanying manuscript.[16]

Prodrug Development. Our Target Product Profile called for an injectable formulation for treatment of seriously ill patients with an anticipated dose >1 g per day. We thus required high solubility (>20 mg/mL) in a vehicle suitable for injection. **ACHN-975** met this goal via the basic amine and has a solubility of >50 mg/mL at pH 5.5. Our second lead, **26** has a solubility of 1 mg/mL at pH 7.4 but does not increase at lower pH. The basic HPCD formulation used for PK and CV studies would not be a cceptable for further development, due to instability of the hydroxamate at elevated pH. We thus undertook the development of a phosphate prodrug to increase solubility.[16] The synthesis of this prodrug is illustrated in Scheme 2.
Prodrug **55** was soluble at >30 mg/mL at pH 6.4 in 0.9% saline, a formulation that allowed dosing of rats up to 500 mg/kg. The pharmacokinetics of **55** were measured in rats and compared to direct dosing of active drug. The results are shown in Figure 5 and Table 5. The phosphate converted rapidly to active drug with a half-life of 2.4 minutes. Bioavailability of active drug from the prodrug was 100%. Based on these results, **55** was chosen for further development.

Table 4. Pharmacokinetic Parameters

Compound	species	Dose (mg/kg)	AUC 0-∞ (μg*h/mL)	Cl (L/hr/kg)	Vss (L/kg)	PPB (% free)[c]	freeAUC:MIC5 ratio
ACHN-975	SD rat	10[a]	12	0.83	0.82	13	4.1
4		5[a]	2.1	2.4	1.70	51	0.53
9		10[b]	5.1	1.9	0.73	32	0.82
10		10[b]	7.7	1.3	0.48	32	0.86
12		10[a]		3.5	0.95	49	2.6
14		10[a]	16	0.63	0.27	40	0.21
15		10[a]	4.8	2.1	0.46	42	0.50
22		5[b]	1.4	3.6	0.91	31	0.24
23		10[b]	4.4	2.3	1.0	23	0.35
24		10[b]	4.6	2.2	0.68	20	0.37
26	SD rat	10[b]	8.1	1.1	0.34	25	0.85
	dog	10[b]	11.7	0.86	0.38	37	NA
	monkey[d]	10[b]	8.2	1.3	0.57	31	NA

[a] formulated in A5D: 2.5% dextrose in 20 mM acetate buffer, pH 5. [b] formulated in 20% HPCD 20% hydroxypropyl cyclodextrin, 250 mM Tris, in water, pH 9. [c] determined by ultracentrifugation.[d] Cynomolgus monkey.

Prodrug Rat CV Safety. As a final evaluation prior to initiating IND-enabling studies on **55**, we re-tested the prodrug in the rat CV safety model. Given its increased solubility, a simple 0.9% saline formulation was used. Surprisingly, dosing of this prodrug resulted in the same CV effects observed upon dosing the basic compounds,

resulting in a CV safety window of <30-fold. The underlying cause for the different outcomes is not known.

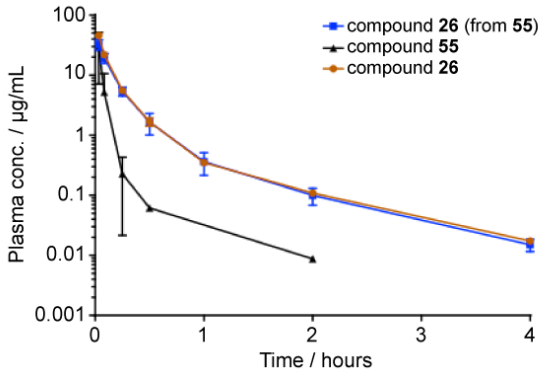

Figure 5. Figure 5. Pharmacokinetic profiles of **26**, **55**, and **26** from **55** in SD rat.

Table 5. Pharmacokinetic Parameters of **26**, **55**, and **26** from **55** in SD Rat.

Compound (dose mg/kg)	Cmax (µg/mL)	AUC AUC 0-∞ (µg*h/mL)	$T_{1/2}$ (h)	Cl (L/h/kg)	Vss (L/kg)
26 (12)	46	7.8	0.7	1.5	0.32
55 (10)	29	3.4	0.04	4.3	0.12
26 from **55**	25	5.6	0.7	-	-

Chemistry. The synthesis of the methyl substituted thietane head began by addition of $LiMe_2Cu$ to olefin **30** with $BF_3{\cdot}Et_2O$ as a promoter (Scheme 1). We relied on an Evans azide transfer scheme to set the amino stereocenter. The sulfide was oxidized to sulfone **35**, which was converted to amine **38** through a standard 3-step sequence. Coupling to tail **39** and treatment with hydroxylamine provided analog **23**.

Conjugate addition of groups other than methyl to olefin **30** failed to provide any product. Thus, to expand the SAR at this position, we executed an Ireland-Claisen reaction to install a vinyl group that could be further functionalized by reduction or cyclopropanation to provide analogs **24** and **25**, respectively.

Synthesis of the methoxy substituted thietane required a modification of our standard route, illustrated in Scheme 2. We discovered that hydroxamate formation from a methyl ester in the final step resulted in racemization of the α-stereocenter. We thus developed a route in which a protected hydroxylamine was coupled to acid **50**, then carried through hydrogenation of the azide and coupling to the fully elaborated tail **53** to afford protected prodrug **54**. The protecting groups were removed with sequentially with TMSBr and HCl to afford prodrug **55**, which could be conveniently purified by precipitation.

Conclusions

ACHN-975 is the first LpxC inhibitor to be tested in humans. A Phase-I clinical trial revealed transient C_{max}-associated hypotension without concomitant tachycardia as a DLT that would limit its utility as a drug. We further optimized LpxC inhibitors for enzyme potency, antibacterial activity, pharmacokinetics, and therapeutic window in a rat CV safety assay. We discovered that compounds from this class with a basic pK_a > 6.5 all displayed an unacceptably low TW of <30-fold. Extensive investigation into the mechanism of this unusual CV effect failed to identify a single molecular target responsible for the observed effect *in vivo*. It remains possible that weak activity against several targets causes the effect. However, given the diversity of structures that show the same effect (including additional data not shown), we believe it unlikely that they all act on the same target(s). Rather we believe it to be a nonspecific effect of these basic amines. This conclusion is further supported by the CV data for **28**, the enantiomer of **ACHN-975**, which displays and identical MTC. We chose **26** for further investigation based on its favorable overall profile, and developed a solubility-enhancing phosphate prodrug that provided rapid conversion to parent. Sadly, the final lead prodrug compound, when tested in the rat CV safety assay (formulated in A5D) demonstrated unacceptable CV toxicity, in stark contrast to the results we obtained dosing the parent compound in an HPCD formulation. The cause for this discrepancy is still not understood.

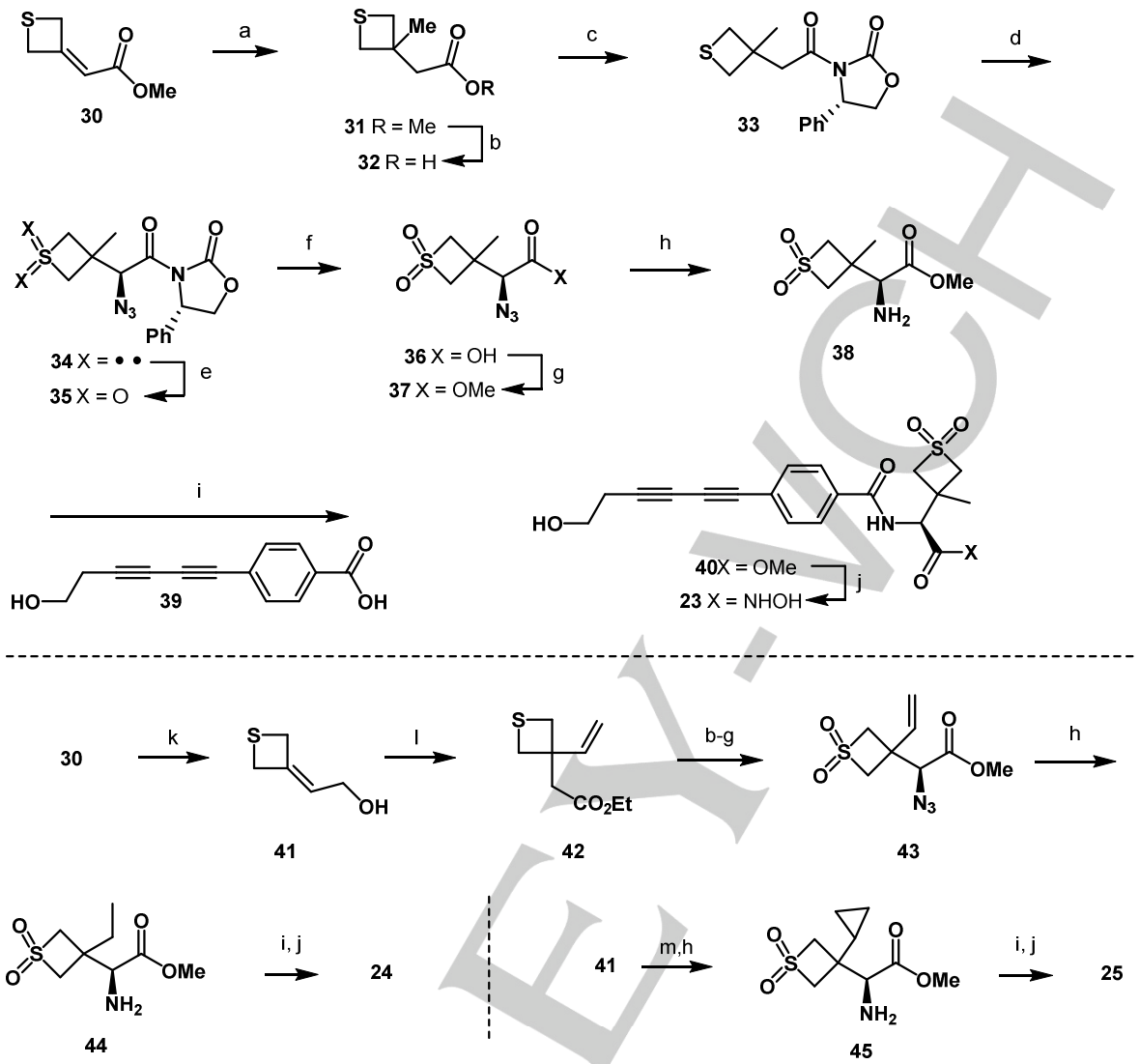

Scheme 1. Synthesis of carbon-substituted thietane-Headgroup LpxC Inhibitors (a) $LiMe_2Cu$, $BF_3{\cdot}Et_2O$, Et_2O, –78 °C to 0 °C, 88%; (b) 1M NaOH, THF, MeOH, 97%; (c) PivCl, TEA, THF, –15 °C then Li(*S*)-(+)-4-phenyl-2-oxazolidinone, –78 °C to 0 °C, 67%; (d) NaHMDS, THF, –78 °C then $TrisylN_3$, 80%; (e) AcOOH, THF, H_2O, 0 °C; (f) LiOOH, THF, H_2O, –5 °C; (g) TMS-diazomethane, DCM, MeOH; quant, 3 steps; (h) H_2, Pd·C, $Pd(OH)_2$·C, EtOAc, MeOH; quant; (i) **39**, HATU, DIPEA, DMF; (j) 50% aq. NH_2OH, iPrOH, 0 °C; (k) DIBALH, PhMe, –78 °C, 95%; (l) triethyl orthoacetate, propionic acid, PhMe, μW 175–180 °C, 1.2 h, 78%; (m) CH_2N_2, $Pd(OAc)_2$, Et_2O, 88%.

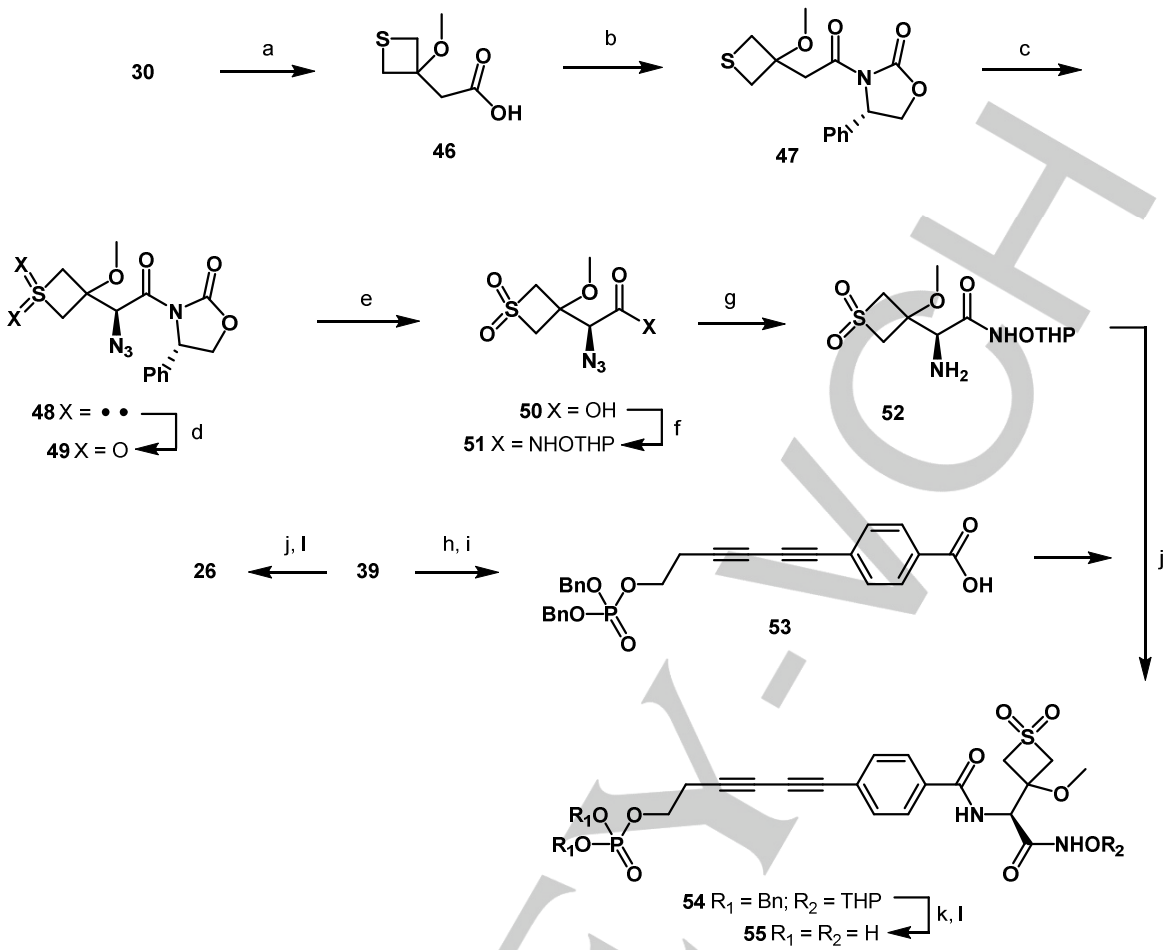

Scheme 2. Synthesis of Methoxy-thietane Head Group and Prodrug **55**. (a) NaOMe, MeOH, then water, 65%; (b) PivCl, TEA, THF, –15 ℃ then (*S*)-(+)-4-phenyl-2-oxazolidinone, LiCl, –10 ℃ to RT, 62%; (c) KHMDS, THF, –65 ℃ then TrisylN$_3$, 62%; (d) $RuCl_3 \cdot 3H_2O$, $NaIO_4$, MeCN, 86%; (e) LiOOH, THF, H_2O, –10 ℃, 85%; (f) H_2NOTHP, DIC, THF; (g) PPh_3, THF, water, 68%, two steps; (h) dibenzyl N,N-diisopropylphosphoramidite, tetrazole, MeCN; (i) H_2O_2, 38%, two steps; (j) HATU, DIPEA, DMF, 58%; (k) N,O-bis(trimethylsilyl)acetamide, TMSBr, DCM; (l) HCl, MeOH, 50%, two steps; (m) **52**, HATU, DIPEA, DMF; (n) HCl, MeCN, 25%, two steps.

Experimental Section

Chemistry. All final compound for biological assay were determined to be >95% by HPLC-MS. All commercially available solvents and reagents were used as received.

Compound **1** is described in WO2008154642[18]; Compounds **2**, **3**, **5**, **9, 39** are described in WO2013170030[19]; Compounds **6, 8** are described in WO2012154204[20]; Compounds **4**, **10**, **11**, **12** are described in WO2014165075[21]; Compounds **7**, **14**, are described in WO2017223349[22]

Additional Schemes and Procedures for preparation of **13, 15, 17–19, 23–26** and **ACHN-975** are provided in the SI.

2-(3-methoxythietan-3-yl)acetic acid (**46**). A reactor with an overhead stirrer was charged sequentially with methanol (125 L, 5 volumes), methyl 2-(thietan-3-ylidene)acetate (25.0 Kg, 173.4 mol, 1 eq.) and 30% NaOMe (53.1 Kg, 1.7 eq, 2.12 weight eq.). The mixture was then stirred at 50 ℃ for 2 hrs, at which time TLC and GC indicated complete consumption of starting material. The reaction is then cooled to 10 ℃, followed by addition of water (250 L, 10 volumes) in portions, maintaining the temperature ≤ 10 ℃. Upon completion of addition, the mixture was maintained at 20 ℃ for 2 h, The MeOH is removed under reduced pressure and the aq phase washed with EtOAc (1 X 200 L, 2 X 100 L). The aq phase is then acidified to pH 1–2 with 12N HCl, and extracted with EtOAc (1 X 100 L, 2 X 50 L). The combined organic phases were washed with brine (2 X 50 L), dried (Na_2SO_4), filtered and concentrated to afford 27 Kg (65%) of the title compound as a yellow solid: ^{1}H NMR 400 MHz $CDCl_3$ δ 7.59-7.57 (m, 1H), 6.95-9.93 (m, 1H), 4.23-4.18 (m, 3H), 4.04 (s, 2H), 3.97 (s, 3H), 1.29-1.26 (m, 3H).

(S)-3-(2-(3-methoxythietan-3-yl)acetyl)-4-phenyloxazolidin-2-one (**47**). A reactor with overhead stirrer was charged with THF (30 L, 20.0 volumes), 2-(3-methoxythietan-3-yl)acetic acid (1.64 Kg, 10.1 mol, 1.1 eq), and cooled to –10 ℃. Pivaloyl chloride (1.22 Kg, 10.1 mol, 1.1 eq) and triethyl amine (2.42 Kg, 23.9 mol, 2.6 eq) were charged sequentially at –10 ℃ and the mixture held at –10 ℃ for 3h. (*S*)-4-phenyloxazolidin-2-one (1.5 Kg, 9.19 mol, 1.00 eq.) and LiCl (456 g, 10.8 mol, 1.17 eq.) were added sequentially at –10 ℃. The mixture allowed stirred at 10–20 ℃ for 16 h. The mixture was cooled

to –10 °C, then water (10 L) was added. The mixture was extracted with EtOAc (2 X 10 L), the combined organic phases were washed with brine (1 X 10 L) and concentrated under vacuum to a solid. The product from 3 batches was combine to afford 7.1 Kg (62%) of the title compound as an off-white solid. ^{1}H NMR 400 MHz $CDCl_3$ δ 7.29-7.38 (m, 5H), 5.44-5.47 (m, 1H), 4.69 (t, *J* = 8.6 Hz, 1H), 4.26-4.29 (m, 1H), 3.73 (s, 2H), 3.63 (t, *J* = 9.6 Hz, 1H), 3.26 (s, 3H), 3.08-3.11 (m, 2H).

(*S*)-3-((S)-2-azido-2-(3-methoxythietan-3-yl)acetyl)-4-phenyloxazolidin-2-one (**48**). A reactor with an overhead stirrer was charged with THF (20 L, 13.3 volumes) and (*S*)-3-(2-(3-methoxythietan-3-yl)acetyl)-4-phenyloxazolidin-2-one (1.5 Kg, 4.88 mol, 1.00 eq.). The solution was cooled to –65 °C then KHMDS (5.37 L of a 1.0M solution in THF, 5.37 mol, 1.1 eq) was slowly added, then the solution held at –65 °C for 1 h. A solution of trisyl azide (1.81 Kg, 5.86 mol, 1.2 eq.) in THF (4 L) was added at –65 °C and the mixture held at that temperature for 1 h. Acetic acid (1.76 Kg, 29.3 mol, 6.00 eq.) and Me_4NOAc (2.6 Kg, 19.5 mol, 4 eq.) were added sequentially. The mixture was allowed to warm to 20 °C and held for 16 h. The mixture was diluted with water (10 L) and EtOAc (10 L), and the phases separated. The aq phase was extracted with EtOAc (10 L), and the combined organic phases were washed with sat. aq. $NaHCO_3$. The organic phase was concentrated under vacuum < 45 °C to a solid. The product from two batches was combined and slurried with EtOH (15 L) for 2 h. The solid was collected by filtration, dried under vacuum to afford 4.5 Kg (62%) of the title compound as an off-white solid: ^{1}H NMR 400 MHz $CDCl_3$ δ 7.37-7.42 (m, 3H), 7.31-7.33 (m, 2H), 5.55 (s, 1H), 5.45-5.48 (m, 1H), 4.74 (t, *J* = 8.8 Hz, 1H), 4.33-4.36 (m, 1H), 3.41-3.51 (m, 8H).

(*S*)-3-((S)-2-azido-2-(3-methoxy-1,1-dioxidothietan-3-yl)acetyl)-4-phenyloxazolidin-2-one (**49**). A reactor with an overhead stirrer was charged sequentially with MeCN (3.5 L, 7.0 volumes) and s(*S*)-3-((S)-2-azido-2-(3-methoxythietan-3-yl)acetyl)-4-phenyloxazolidin-2-one (0.50 Kg, 1.4 mol, 1.0 eq.) water (3.5 L, 7.0 volumes), and $RuCl_3{\cdot}3H_2O$ (0.75 g, 2.87 mol, 0.002 eq.). $NaIO_4$ (629 g, 2.94 mol, 2.05 eq.) was added in portions, maintaining the internal temperature ≤ 30 °C. The mixture was stirred for 3 h. Aq. $NaHCO_3$ (0.5 L) was added and the mixture stirred for 15 min. The mixture was extracted with DCM (2 X 2 L) and filtered. The filtrate was extracted with DCM (2 L). The combined organic phases were washed with $Na_2S_2O_3$, brine, dried and evaporated under vacuum at 40°C to afford a solid. The solid was slurried with EtOH (2 L) for 1h, the solid was collected by filtration, dried under vacuum to afford 470 g (86%) of the title compounds as a colorless solid: ^{1}H NMR 400 MHz $CDCl_3$ δ 7.41-7.45 (m, 3H), 7.30-7.39 (m, 2H), 5.91 (s, 1H), 5.47-5.50 (m, 1H), 4.80 (t, *J* = 9.0 Hz, 1H), 4.43-4.51 (m, 3H), 4.22-4.40 (m, 2H), 3.46 (s, 3H).

(*S*)-2-azido-2-(3-methoxy-1,1-dioxidothietan-3-yl)acetic acid (**49**). A solution of (*S*)-3-((S)-2-azido-2-(3-methoxy-1,1-dioxidothietan-3-yl)acetyl)-4-phenyloxazolidin-2-one (500 g, 1.31 mol), THF (11.25 L) and H_2O (3.75 L) was cooled to –10 °C and 30% H_2O_2 (806 mL, 7.89 mol) was added. The mixture was stirred for 60 min, at which time LiOH (69.0 g, 2.88 mol) in H_2O (750 mL) was added, and the solution was stirred at –10 °C for 0.5 h. The reaction mixture was quenched by the addition of 10% $Na_2S_2O_3$ in H_2O (9.0 L) and warmed to room temperature. The mixture was extracted twice with DCM (15 L, 11 L) and the aqueous solution was acidified to pH ~1 with 6N HCL and extracted with 15% iPrOH in DCM (6 x 8 L). The organic layers were concentrated to minimum volume and filtered to provide white solid which was removed by filtration. The filtrate was concentrated to provide (*S*)-2-azido-2-(3-methoxy-1,1-dioxidothietan-3-yl)acetic acid (**2**) (261 g, 85%) as an off-white solid.

(2*S*)-2-amino-2-(3-methoxy-1,1-dioxidothietan-3-yl)-N-((tetrahydro-2H-pyran-2-yl)oxy)acetamide (**50**). (*S*)-2-azido-2-(3-methoxy-1,1-dioxidothietan-3-yl)acetic acid (510 g, 2.17 mol) was dissolved in THF (500 ml) and cooled (T_{int}= –8.5 °C). O-(tetrahydro-2H-pyran-2-yl)hydroxylamine (254.1 g, 2.17 mol, 1.0 eq.) was added and the mixture was stirred for 10 min. N,N′-Diisopropylcarbodiimide (273.9 g, 2.17 mol, 1.0 eq.) was then added dropwise, and the mixture was stirred for 0.5 h, at which time it was filtered and triphenylphosphine (1023 g, 3.91 mol, 1.8 eq) was added to the filtrate and stirred for 1 h. Water (780 mL, 43.4 mol, 20.0 eq.) was added, and the mixture was heated to 70 °C and stirred overnight. The cooled solution was evaporated and water (5 L) was added to the residue and stirred at 60 °C for 1 h. The cooled solution was filtered, and sodium chloride (300 g) was added. Extraction with 16% iPrOH in $CHCl_3$ (5 x 4 L) and evaporation of the combined solvent followed by drying under high vacuum, afforded (2*S*)-2-amino-2-(3-methoxy-1,1-dioxidothietan-3-yl)-N-((tetrahydro-2H-pyran-2-yl)oxy)acetamide as an off-white foam (458 g, 68 %).

4-(6-((bis(benzyloxy)phosphoryl)oxy)hexa-1,3-diyn-1-yl)benzoic acid (**53**). To a solution of compound **39** (1000 g, 4.67 mol, 1.00 equiv) in acetonitrile (12.5 L) was added tetrazole (655 g, 9.35 mol, 2 equiv) and the resultant mixture was stirred for 30 min. To this was added dibenzyl N,N-diisopropylphosphoramidite (1937 g , 5.61 mol, 1.2 equiv) drop wise at 15–20 °C and the reaction mixture was stirred at RT for additional 16 h. The reaction mixture was cooled to 0 °C in an ice/water bath and 30% hydrogen peroxide (5.29 L, 46.72 mol, 10 equiv) was added drop wise (*Note: highly exothermic reaction during initial addition*) and stirred for 1 h. The mixture was quenched with 5% HCl solution (pH ~2) and diluted with ethyl acetate (20 L) and brine (4 L). This was stirred for 30 min and then filtered through a pad of Celite®. The organic layer was separated from the filtrate and washed with brine (2 X 2000 ml) and dried (Na_2SO_4). The solvent was concentrated under vacuum and the crude compound obtained was diluted with acetonitrile (3000 mL), stirred for 2 h at 0 °C and filtered. The solid obtained was further slurred in methanol (2000 mL) for 1 h, filtered and dried under vacuum to afford compound **53** (856 g, 38%**)** as off white solid.

dibenzyl (6-(4-(((1S)-1-(3-methoxy-1,1-dioxidothietan-3-yl)-2-oxo-2-(((tetrahydro-2H-pyran-2-yl)oxy)amino)ethyl)carbamoyl)phenyl)hexa-3,5-diyn-1-yl) phosphate (**54**). (2*S*)-2-amino-2-(3-methoxy-1,1-dioxidothietan-3-yl)-N-((tetrahydro-2H-pyran-2-yl)oxy)acetamide (**4**) (458.5 g, 1.49 mol, 1.30 eq.) was dissolved DMF (4.5 L) at –5 °C and 4-(6-((bis(benzyloxy)phosphoryl)oxy)hexa-1,3-diyn-1-yl)benzoic acid (**5**) (540 g, 1.14 mol, 1.00 eq.) was added and stirred for 10 min. DIEA (5.95 L, 3.43 mol, 3.00 eq.) was then added in one portion followed by HATU (477 g, 1.26 mol, 1.11 eq.) in one portion (T_{int} = 11 °C). The resulting mixture was stirred for 0.5 h after which time the reaction mixture was diluted with H_2O (8 L) and extracted with EtOAc (8 L). The org layer was concentrated *in vacuo* to provide a dark green oil (~1.2 L) which was purified by flash chromatography on silica gel, eluting with 0 – 90 % EtOAc in hexane to provide **81** (509 g, 58 %) as a greenish solid.

(*S*)-6-(4-((2-(hydroxyamino)-1-(3-methoxy-1,1-dioxidothietan-3-yl)-2-oxoethyl)carbamoyl)phenyl)hexa-3,5-diyn-1-yl dihydrogen phosphate (**55**). Dibenzyl (6-(4-((1-(3-methoxy-1,1-dioxidothietan-3-yl)-2-oxo-2-(((tetrahydro-2H-pyran-2-yl)oxy)amino)ethyl)carbamoyl)phenyl)hexa-3,5-diyn-1-yl) phosphate **54** (383.3 g, 0.5 mol, 1.00 eq.) in DCM (4 L) was cooled to 0 °C, and (N,O-bis(trimethylsilyl)acetamide) (510.3 g, 2.5 mol, 5.00 eq.) was added dropwise followed by TMSBr (307 g, 2.0 mol, 4.00 eq). The mixture was stirred at 0 °C for 40 min, quenched by the addition of Et_3N (703 mL, 5.06 mol) and then stirred for 5 min. The mixture was evaporated, and the residue was taken up in MTBE (4.0 L), stirred for 5 min and filtered. The cake was rinsed with MTBE (2 L). The combined MTBE layers were diluted with MeOH (1 L) followed by DCM (1 L). The mixture was concentrated under reduced pressure, and the residue was partitioned between water (4 L) and EtOAc (4 L). The aqueous layer

was then acidified with 6M HCL (60 ml) and extracted with 2-methyl THF (6 L). The organic layer was washed with H_2O (2 X 40 mL), 6N HCL (2 X 40 mL), dried over $MgSO_4$ and evaporated to provide 6-(4-(((1S)-1-(3-methoxy-1,1-dioxidothietan-3-yl)-2-oxo-2-(((tetrahydro-2H-pyran-2-yl)oxy)amino)ethyl)carbamoyl)phenyl)hexa-3,5-diyn-1-yl dihydrogen phosphate as a tan solid (191.2 g, which was used directly for the next step without further purification.

The product from above was dissolved in MeOH (1.9 L) and 4M HCl (180 mL) was added. The mixture was stirred for 15 min and evaporated to give crude material which was dissolved in H_2O (12 L). The mixture was washed with EtOAc (12 L) / toluene (2.5 L). The aqueous layer was then extracted with two portions of methyl THF (20 L + 12 L). The combined organic layers were dried ($MgSO_4$), stirring for 1 h. The mixture was filtered then evaporated to give a tan solid (123 g, 96.5 % pure). The solid was dissolved in H_2O (11 L) and washed with 16% iPrOH in CH_3CL (4 x 5 L). The aqueous layer was then extracted with EtOAc (10 x 6 L) and the combined organic layers were evaporated to afford (S)-6-(4-((2-(hydroxyamino)-1-(3-methoxy-1,1-dioxidothietan-3-yl)-2-oxoethyl)carbamoyl)phenyl)hexa-3,5-diyn-1-yl dihydrogen phosphate **55** as an off-white solid (92 g, 50 % yield). MS: m/z for $C_{19}H_{21}N_2O_{10}PS$ 500.4, found $[M+H]^+$ 501.3.

Measurement of Antibacterial Activity. MICs were determined by broth microdilution according to guidelines established by the Clinical and Laboratory Standards Institute.[22] Compounds were serially diluted in two-fold increments in 100% DMSO, then diluted 10-fold in water. Inocula were prepared from cells streaked onto Mueller Hinton agar (MHA) and grown at 35 °C overnight. 10 uL of antibiotic solution was mixed with 90 uL of inoculum in cation-adjusted Mueller Hinton broth in 96-well assay plates, with a final inoculum of approximately 5 x 10^4 cells/well. When included, PMBN was diluted in broth prior to addition of cells, to a final assay concentration of 8 µg/mL. After incubation of assay plates at 35 °C for 18-20 hours, the lowest concentration of antibiotic that prevented visible growth was recorded as the MIC.

P. aeruginosa LpxC protein purification**.** A IPTG-inducible expression plasmid for WT *P. aeruginosa* LpxC with an N-terminal 6-His tag was transformed into Rosetta™(DE3)pLysS *E. coli* cells (Novagen) for protein expression. Cells containing the expression plasmid were grown in 50 µg/mL kanamycin and 17 µg/mL chloramphenicol at 30 °C. The cultures were induced with 0.5 mM IPTG and 10 µM $Zn(acetate)_2$ at an OD_{600} of 0.5 absorbance units. After growth at 30 °C for an additional 2.5 h, the cells were harvested by centrifugation at 10,500 rpm in a JA10.5 rotor for 15 min. Afterwards the supernatant was removed, the cells resuspended in buffer A [25 mM Tris-HCl, 100 mM NaCl, 100 µM $Zn(acetate)_2$, 5 mM imidazole, and pH 8.0], and the resuspension stored at -80 °C.

The resuspended cells were lysed using an microfluidzer (Microfluidics™ LM10; 16,000 psi, 4 passages). The lysate was centrifuged at 18,000 rpm in a JA25.5 rotor for 45 min and the resulting supernatant was filtered through a 0.45 uM syringe-operated filter. The filtered supernatant was applied via gravity flow to a 3 mL HisPur™ (Thermo Scientific). The column was washed with approximately 80 mL of buffer A. The bound enzyme was eluted with 20 mL of buffer B 25 mM Tris-HCl, 100 mM NaCl, 100 µM $Zn(acetate)_2$, 150 mM imidazole, and pH 8.0). The elution volume was dialyzed overnight at 4 C into 4L of storage buffer (25 mM imidazole, 100 mM KCl, 2 mM DTT, 20% Glycerol, and pH 7.0). The enzyme solution was then filtered through a 0.2 µm syringe-operated filter, aliquoted, and stored at –80 °C to be later used in the LpxC IC_{50} assay and for x-ray crystallography studies. The presence of the desired enzyme and final purity was estimated by SDS-PAGE to be >95%. The concentration of total enzyme was determined by A_{280} using a calculated extinction coefficient of 15,390 $M^{-1}cm^{-1}$ or by Bradford assay.

LpxC Enzyme IC_{50} Assay. The LpxC enzyme inhibition assay was adapted from the method detailed by Hale et al. and uses recombinant *P. aeruginosa* LpxC purified from *E. coli*.[24] Test compounds previously dissolved in DMSO are diluted to a 10X stock concentration in water such that the final DMSO concentration in the assay is less than 1%. 3 µL of 10X test compound is then aliquoted in 3-fold dilutions across the row of a 96-well plate. 24 µL of a buffered LpxC enzyme-containing solution (fresh enzyme is obtained from a –80 °C previously aliquoted stock) is then added to the test compound dilutions. The enzyme and test compound are allowed to incubate for 10 minutes at room temperature. To initiate the reaction, 3 µL of 400 µM UDP-3-O-(R-3-hydroxydecanoyl)-N-acetylglucosamine (CAS# 953426-26-1; obtained from Beijing Honghui Meditech Co., Ltd) is added. The final reaction conditions of the assay are 10 mM sodium phosphate, pH 7.5, 0.005% Triton X-100, 1 mM TCEP, 40 µM UDP-3-O-(R-3-hydroxydecanoyl)-N-acetylglucosamine, and 10 µM $Zn(acetate)_2$. The final expected concentration of catalytically active LpxC was estimated to be approximately 0.1 nM. The reaction was allowed to progress to approximately 20% completion in the absence of test compound over 8 hours at which point 3 µL of 1 M HCl is added to the reaction to terminate enzyme activity.

The progress of the reaction at each concentration of test compound was measured using LC/MS. For LC/MS analysis, 20 µL of quenched reaction solution was injected onto Agilent 1290 UPLC system using a Kinetex C18 100A, 2.1x50 mm, 2.6 µm column (Phenomenex). Reaction product and substrate were eluted into the mass spectrometer (Agilent 6120) with a gradient starting at 16% Acetonitrile, 84% 20 mM Ammonium Acetate, pH 6.7 to 20% Acetonitrile, 80% 20 mM Ammonium Acetate, pH 6.7 over 1.75 minutes. Product was quantified by monitoring abundance of m/z 734.3 and the substrate was quantified by monitoring abundance of m/z 776.3 both in negative ion mode. While the substrate peak remains stable over time, the product of the LpxC reaction is known to slowly rearrange over time resulting in the formation of two peaks in the mass spectrum. Both product peaks, in addition to the substrate peak, are integrated and used to compute the percent reaction progress at each test compound concentration. The percent reaction progress at zero test compound is used to normalize the data at each test compound concentration. A 3-parameter fit is used to fit the relationship between the normalized reaction progress and the test compound concentration, yielding a fitted IC_{50} value. The lower limit of detection for the IC_{50} value in this assay is less than 0.3 nM.

Anesthetized Rat Methodology: All animals studies were performed with the approval of the Institutional Animal Care and Use Committee at Plato Biopharma, Inc. and in compliance with the Guide for the Care and Use of Laboratory Animals. Four male Sprague Dawley rats (approximately 7 weeks of age) per study were anesthetized using inhaled isoflurane (ISO) on spontaneous nose-cone rebreathing with 2.0% ISO in 100% O_2 during surgery, and 1.5% ISO for maintenance. Body temperature was maintained with rectal probe-controlled heating pads. Cannulae were surgically implanted in the femoral artery, vein, and jugular vein for blood pressure measurement, IV infusion of test article and blood sampling, respectively. Test articles were delivered by intravenous infusion at a rate of 10 mL/kg/h in either HPCD/Tris (20% HPCD, 250 mM Tris) or A5D2.5 (2.5% Dextrose in 20 mM Acetate buffer). In dose escalation (DE) studies, vehicle and 3 dose levels were infused for 30 minutes per dose level. In maximum tolerated dose (MTD) studies, vehicle was infused for 30 minutes followed by one dose level of test article for 60 minutes. Blood samples were drawn to assess plasma levels with the following time points: DE studies: @30, 60 90, and 120 minutes of infusion, and 2, 6, 12 and 30 minutes post-infusion cessation; MTD studies: @30, 45, 60, 75, 90 minutes of infusion, and 2, 6, 12, and 30 minutes. Steady-state and time-dependent hemodynamic parameters (mean arterial pressure

(MAP), systolic and diastolic blood pressure (SBP, DBP), and heart rate (HR) were collected and expressed as minute averages over the study duration. Parameters were expressed as actual values (both individual and mean) and as percent change from vehicle where the final 10 minutes of the vehicle infusion data were averaged for the baseline value. Test article plasma levels were expressed as total concentrations and free concentrations using the protein binding data for the test article per time point. Stopping criteria for test article infusion of MAP decrease of 30 mmHg or 30% decrease in HR for 2 continuous minutes were established. All animals were euthanized under anesthesia at the end of the study after inspection of the infusion catheter tip site via laparotomy.

Acknowledgements

This work was supported by The Defense Threat Reduction Agency, Department of Defense, under Contract No. HDTRA107C0079, the Military Medical Research and Development Program, Defense Health Program, Department of Defense, under Grant No. W81XWH122000040 and by the National Institute of Allergy and Infectious Diseases, National Institutes of Health, Department of Health and Human Services, under Contract No. HHSN272201500009C. We thank Phil Patten, J. Kevin Judice, and Marc Navre for leadership and guidance.

Keywords: Amines, Antibiotics, Inhibitors, LpxC, Prodrugs, Pseudomonas, Zwitterions

References:

[1] J. Burnham, M. Olsen, M. Kollef, *Infect. Control Hosp. Epidemiol.* **2019,** *40*, 112-113.
[2] Centers for Disease Control and Prevention. (**2013**). *Antibiotic resistance threats in the United States, 2013*. Retrieved Feb. 27, 2019, from CDC website: www.cdc.gov/drugresistance/threat-report-2013.
[3] L. Chen, R. Todd, J. Kiehlbauch, M. Walters, A. Kallen, *MMWR Morb. Mortal Wkly. Rep.* **2017**, *66*, 33.
[4] R. Tommasi, R. Iyer, A. A. Miller, *ACS Infect. Dis.* **2018**, *4*, 686-695..
[5] D. J., Payne, M. N., Gwynn, D. J. Holmes, D. L. Pompliano, *Nat. Rev. Drug Disc.* **2007**, *6*, 29-40.
[6] C. R. Raetz, C. M. Reynolds, M. T. Trent, R. E. Bishop, *Ann. Rev. Biochem.* **2007**, *76*, 295-329.
[7] A. L. Erwin, *Cold Spring Harb. Perspect. Med.* **2016**, *6*, a025304.
[8] F. Liu, S. Ma, *Mini-Rev. Med. Chem.* **2018**, *18*, 310-323.
[9] M. Vaara, *Microbiol. Rev.* **1992**, *56*, 395-411.
[10] O. Lomovskaya, A. Lee, K. Hoshino, H. Ishida, A. Mistry, M. S. Warren, E. Boyer, S. Chamberland, V. J. Lee, *Antimicrob. Agents Chemother.* **1999**, *43*, 1340-1346.
[11] Davies, B. I., *Antimicrob. Agents Chemother.* **1990**, *25*, 471-472.
[12] L. Xingrong, M. Wright, C. E. Hop, *J. Med. Chem., **2014**, 57*(20), 8238-8248.
[13] M. F. Richter,B. S. Drown, A. P. Riley, A. Garcia, T. Shirai, R. L. Svec, P. J. Hergenrother, *Nature,* **2017**, *545*, 299-304.
[14] M. F. Richter, P. J. Hergenrother, *Annals of the New York Academy of Sciences,* **2019**, *1435*, 18-38.
[15] G. F. Smith, *Progress Med. Chem.* **2011**, *50*, 1-47.
[16] K. Krause, C. M. Haglund, C. Hebner, A. W. Serio, G. Lee, V. Nieto, F. Cohen, T. R. Kane, T. Machajewski, D. J. Hildebrandt, A. Burek, L. D. Andrews, E. Armstrong, L. Swem, A. Jubb, R. T. Cirz. Manuscript Accepted.
[17] V. Stella, R. Borchardt, M. Hageman, R. Oliyai, H. Maag, J. Tilley, *Prodrugs: Challenges and Rewards Part 1 and 2*. Springer, New York, NY, **2007**.
[18] H. Moser, Q. Lu, P. A. Patten, D. Wang, R. Kasar, S. Kaldor, B. D. Patterson (Achaogen), WO2008154642, **2008**.
[19] B. D. Patterson, Q. Lu, J. B. Aggen, P. Dozzo, R. A. Kasar, M. S. Linsell, T. R. Kane, M. J. Gliedt, D. J. Hildebrandt, G. A. McEnroe, F. Cohen (Achaogen), WO2013170030, **2013**.
[20] R. Kasar, M. S. Linsell, J. B. Aggen, Q. Lu, D. Wang, T. Church, H. E. Moser, P. A. Patten (Achaogen), WO2012154204, **2012**.
[21] M. S. Linsell, J. B. Aggen, P. Dozzo, D. J. Hildebrandt, F. Cohen, R. A. Kasar, T. R. Kane, M. J. Gliedt, G. A. McEnroe (Achaogen), WO2014165075, **2014**.
[22] F. Cohen, A. W. Konradi, T. A. Choi, T. Machajewski, T. R. Kane, D. J. Hildebrandt (Achaogen), WO2017223349, **2017**.
[23] CLSI. *Methods for Dilution Antimicrobial Susceptibility Tests for Bacteria That Grow Aerobically; Approved Standard—Tenth* Edition. CLSI document M07-A10. Wayne, PA: Clinical Laboratory Standards Institute; **2015**.
[24] M. R. Hale, P. Hill, S. Lahiri, M. D. Miller, P. Ross, R. Alm, N. Gao, A. Kutschke, M. Johnstone, B. Prince, J. Thresher, W. Yang, *Bioorg. Med. Chem. Lett.* **2013**, *23*, 2362-2367.

10.1002/cmdc.201900287

WILEY-VCH

Entry for the Table of Contents

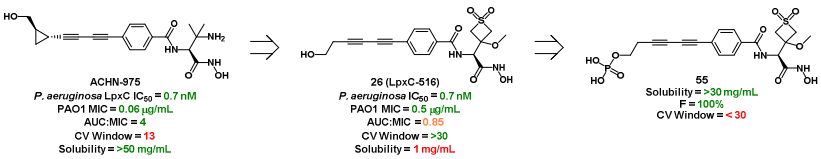

It's not the hydroxamate!: Antibacterial LpxC inhibitors have optimized for enzymatic potency, anti-Pseudomonal activity, pharmacokinetics and cardiovascular safety. We demonstrate that the much-maligned hydroxamic acid is not responsible for the CV toxicity observed with LpxC inhibitors. Development of a phosphate prodrug enabled high solubility and rapid conversion to active drug upon i.v. administration.